Macrophages Are Necessary for Maximal Nuclear Factor-κB Activation in Response to Endotoxin

M. Audrey Koay, Xiang Gao, Mary Kay Washington, Kelly S. Parman, Ruxana T. Sadikot, Timothy S. Blackwell, and John W. Christman

Department of Medicine, Division of Allergy, Pulmonary, and Critical Care Medicine, and Department of Pathology, Vanderbilt University School of Medicine, Nashville; and Department of Veterans Affairs, Nashville, Tennessee

To define the role of macrophages in regulating the lung's response to *Escherichia coli* endotoxin (lipopolysaccharide [LPS]), depletion of macrophages was accomplished by administration of dichloromethylene diphosphonate (clodronate) delivered via intratracheal (IT) and/or intravenous (IV) routes. Clodronate reduced the number of macrophages in lung lavage 48 h after either IT or IV administration, but combined IT+IV clodronate achieved the most profound depletion (90%). Although IT clodronate alone had little effect on the evolution of lung inflammation, combined IT+IV clodronate treatment decreased neutrophilic alveolitis 4 h after exposure to aerosolized LPS by 80% compared with mice treated with empty liposomes. This decrease was associated with impaired activation of nuclear factor (NF)-κB and lower concentrations of tumor necrosis factor (TNF)-α in lung lavage fluid. Combined IT+IV clodronate markedly reduced lung NF-κB activation and the intensity of neutrophilic alveolitis after intraperitoneal (IP) LPS; however, IV clodronate alone had no effect on NF-κB activation in either liver or lung tissue or the development of neutrophilic alveolitis. We conclude that generalized macrophage depletion reduces NF-κB activation, generation of cytokines, and neutrophilic lung inflammation in response to gram negative bacterial endotoxin. These findings define the role of the macrophage as a critical component for initiation of the NF-κB–dependent innate immune response.

Dichloromethylene bisphosphonate (clodronate) is a synthetic bisphosphonate that has been used to selectively eliminate macrophages in various tissues (1, 2). The highly hydrophillic nature of free clodronate precludes its passage through the cell lipid bilayer; therefore, cellular uptake requires incorporation into liposomes (3). Uptake of liposomal-encapsulated clodronate has been demonstrated by monocytes and macrophages and results in selective apoptosis (4–6). Minimal uptake is demonstrated in neutrophils and endothelial cells, but this does not result in apoptosis and liposomal clodronate does not accumulate in T lyphocytes or epithelial cells (4).

Substantial depletion of alveolar macrophages occurs within 24 h of intratracheal (IT) administration of liposomal clodronate and persists for at least 72 h (3, 7). Complete alveolar macrophage reconstitution requires up to 18 d (8). Presumably, reconstitution occurs by recruitment and differentiation of peripheral blood monocytic precursors. In contrast, intravenous (IV) administration of clodronate results in nearly complete elimination of splenic and hepatic macrophages and partial elimination of bone marrow macrophages (1, 2) but effects on pulmonary macrophages have not been reported. We speculated that combined IT+IV administration of clodronate would substantially deplete alveolar and pulmonary interstitial macrophages in addition to globally depleting macrophages in extrapulmonary locations, including the liver.

Liposomal encapsulated clodronate has been exploited in experimental models of autoimmune disease, septic shock, pneumonia, and other inflammatory conditions to study the antimicrobial and immunoregulatory role of macrophages. For example, alveolar macrophage depletion by IT administration of clodronate has a marked impact on the course of bacterial pneumonia (9–12). Models of lung infection consistently demonstrate delayed bacterial clearance, but the effect of macrophage depletion on neutrophilic lung inflammation and cytokine production has been variable (9–12). These studies do not allow distinction between the effects of a persistent or exaggerated inflammatory insult that results from delayed or impaired bacterial clearance versus alteration in the intrinsic lung inflammatory response to the inciting stimulus in macrophage-deficient lungs.

We used models of lung inflammation induced by inhaled and intraperitoneal (IP) injection of *Escherichia coli* lipopolysaccharide (LPS), in which the inciting insult is transient and the inflammatory response is well defined. Our data indicate that macrophages are a critical component of the innate immune response in the lungs that regulate the development of neutrophilic lung inflammation, lung nuclear factor (NF)-κB activation, and production of cytokines and chemokines following administration of LPS.

Materials and Methods

Materials

Clodronate and LPS (*E. coli* serotype 055:B5) were obtained from Sigma (St. Louis, MO). Monoclonal antibodies to mouse F4/80, a macrophage-specific surface marker, and mouse anti-lysosomal antibodies used in immunohistochemistry studies were obtained from Serotec (Raleigh, NC). The double-stranded consensus NF-κB motif, 5′-GATCGAGGGGACTTTCCCTAAAAGC-3′, used in electrophoretic mobility shift assays (EMSA) was obtained from Stratagene (La Jolla, CA). γ-ATP-p32 was obtained from NEN-Dupont (Boston, MA), and T4 kinase and T4 kinase buffer used for oligonucleotide labeling were from New England Biolabs (Beverley, MA). Polyclonal antibodies to RelA (also called p65) and p50 used in performing EMSA supershifts were obtained from Santa Cruz Biotechnology (Santa Cruz, CA). Isoflurane and ketamine were used for animal anesthesia and were obtained from Fort Dodge Animal Health (Fort Dodge, IA).

(*Received in original form October 17, 2001 and in revised form January 14, 2002*)

Address correspondence to: John W. Christman, M.D., Division of Allergy, Pulmonary, and Critical Care Medicine, Vanderbilt University School of Medicine, T-1217 MCN, Nashville, TN 37232-2650. E-mail: john.christman@mcmail.vanderbilt.edu

Abbreviations: bronchoalveolar lavage, BAL; cytokine-induced neutrophil chemoattractant, CINC; electrophoretic mobility shift assay, EMSA; intraperitoneal, IP; intratracheal, IT; intravenous, IV; lipopolysaccharide, LPS; monocyte chemotactic protein, MCP; macrophage inflammatory protein, MIP; nuclear factor-κB, NF-κB; phosphate-buffered saline, PBS; tumor necrosis factor-α, TNF-α.

Am. J. Respir. Cell Mol. Biol. Vol. 26, pp. 572–578, 2002
Internet address: www.atsjournals.org

Liposomal Encapsulation of Clodronate

Eight milligrams of cholesterol were added to 86 mg of egg phosphatidylcholine and the chloroform phase evaporated under helium until a white film remained. Further removal of the chloroform phase was performed under low vacuum in a speedvac Savant concentrator (Holbrook, NY). The clodronate solution was made by dissolving 1.2 g of dichloromethylene diphosphonic acid in 5 ml of sterile phosphate-buffered saline (PBS). Five milliliters of the clodronate solution were added to the liposomes and mixed thoroughly. Empty liposomes were made by the addition of sterile PBS alone. This solution was sonicated and ultra-centrifuged at 10,000 $\times$ g for 1 h at 4°C. The liposomal pellets were then removed and resuspended in PBS, followed by ultra-centrifugation at 10,000 $\times$ g for an hour at 4°C. Subsequently, liposomes were resuspended in 5 ml of sterile PBS, stored at 4°C, and used within 48 h. The final concentration of the liposomal clodronate suspension was 5 mg/ml.

Administration of Liposomal Clodronate

A single dose of liposomal clodronate or liposomal PBS was administered to mice via IT and/or IV routes. Control mice received empty (PBS-containing) liposomes. Mice were sedated with isoflurane and ketamine. Tracheas were exposed by surgical resection and pierced with a 26-gauge needle for IT injections (100 μl). The neck wound was closed with sterile sutures. IV injections (200 μl) were given via tail vein.

Histologic Examinations of Lung and Liver in Clodronate-Treated Mice

Tissue slides of formalin-fixed livers and lungs were stained with anti-mouse monoclonal antibodies to the macrophage surface marker F4/80 antigen and anti-lysosomal antibodies, respectively, for the identification of tissue macrophages. The histology was examined by taking digital images of five consecutive high-power fields. Kupffer cells and pulmonary macrophages were counted by two separate blinded observers. The total macrophage counts were the mean $\pm$ SEM of the average counts from the two reviewers for each treatment group.

Animal Model

C57Bl/6 mice were obtained from Harlan Sprague Laboratories (Indianopolis, IN). Mice were maintained on a 12 h light, 12 h dark cycle; housed in filtered air cages; fed standard chow pellet diet; and had free access to water. Adult mice weighing between 25 and 30 g were used for all experiments. For inhalation exposure, lyophilized *E. coli* LPS was suspended in sterile saline (0.1 mg/ml). LPS solution (7 ml) was delivered as a continuous aerosol with a driving flow rate (8 L/min) that was generated by a small volume nebulizer (Resigard II; Marquest Medical, Englewood, CO) over a standardized 30-min interval. The optimal dose and duration of the LPS aerosol was determined in previous studies (13). Mice were exposed to aerosolized LPS by placing them within a sealed container. Mice were killed 4 h after exposure to aerosolized LPS.

For IP administration, lyophilized *E. coli* LPS was suspended in sterile saline (0.5 mg/ml). LPS (5 μg/g) was administered by a single IP injection. Mice were killed 90 min after LPS injection for determination of hepatic and pulmonary NF-κB activity, and at 24 h for estimation of neutrophilic alveolitis. Mice were euthanized by carbon dioxide inhalation as recommended by the Panel on Euthanasia of the American Veterinary Medical Association.

Bronchoalveolar Lavage Fluid and Tissue Harvesting

Bronchoalveolar lavage (BAL) fluid and tissue samples were collected after death. Mouse tracheas were cannulated with a 20-gauge blunt tip needle attached to a 1-ml syringe, and the lungs were instilled with sterile pyrogen-free physiologic saline until a total lavage volume of 3 ml was collected. Lungs were harvested by resection and tissues were immediately flash frozen in liquid nitrogen and stored at –70°C.

Total and differential cell counts were measured in lung lavage fluid. After centrifugation at 500 $\times$ g for 10 min, the cell pellet was resuspended in 1 ml of 1% bovine serum albumin in sterile physiologic saline. Total cell counts are determined using a grid hemocytometer. Differential cell counts were obtained by staining cytocentrifuge slides with a modified Wright's stain (Diff-Quik; Baxter, Miami, FL) and counting 400 cells in a cross-section.

Extraction of Nuclear Proteins from Tissue Samples

Tissue nuclear proteins were extracted from whole lung by the method of Deryckere (14). A quantity of 50–100 mg of tissue was mechanically homogenized in liquid nitrogen to which 4 ml of buffer A (NaCl 150 mM, HEPES 1 M, NP40, EDTA 0.2 M, phenylmethylsulfonylfluoride 0.1 M) was added. The homogenate was transferred to a 15-ml Falcon tube (Becton Dickinson Labware, Franklin Lakes, NJ) and centrifuged at 850 $\times$ g for 30 s to remove cellular debris. The supernatant was then transferred to a 50-ml Falcon conical and incubated on ice for 5 min before being centrifuged for 10 min at 3,500 $\times$ g. The supernatant was collected as cytoplasmic extract. The pellet was resuspended in 300 μl of buffer B (sterile water, glycerol, HEPES 1 M, NaCl 5 M, $MgCl_2$ 1 M, EDTA 0.2 M, PMSF 0.1 M, DTT1 M, benzamidine 10 mg/ml, pepstatin 1 mg/ml, leupeptin 1 mg/ml, aprotinin 1 mg/ml) and incubated on ice for 30 min. Following a 2-min microcentrifugation at 14,000 rpm, the supernatant was collected as the nuclear extract and frozen at –70°C. Protein concentrations in nuclear and cytoplasmic extracts were determined using the Bradford assay (15).

Oligonucleotide Labeling

Oligonucleotides were labeled using a double-stranded consensus sequence NF-κB and γ-p32-ATP. The reaction was catalyzed with T4 polynucleotide kinase and incubated in 10$\times$ kinase buffer at 37°C for 45 min. The reaction was ceased by heating at 65°C for 10 min. Labeled oligonucleotide was column-purified on Sephadex G-25 columns (Amersham Pharmacia Biotech, Sweden).

Electrophoretic Mobility Shift Assays

Five micrograms of nuclear proteins were incubated with binding buffer on ice for 30 min (specific antibodies for p50 and RelA were added for supershift studies). Oligonucleotide labeled with γ-p32 ($\sim$ 100,000 counts/min) was then added and samples incubated at room temperature for 1 h. Specificity of binding was ascertained using cold competition with an excess of unlabeled NF-κB oligonucleotides. Protein–DNA complexes were separated from the free DNA probe by electrophoresis through 6% polyacrylamide gels run at room temperature at 150 V for 3–4 h. Gels are dried under vacuum on Whatman filter paper in a Bio-Rad Gel-dryer (Bio-Rad, Hercules, CA) and exposed to autoradiographic film.

Cytokine Enzyme-Linked Immunosorbent Assays

Cytokine assays were performed on BAL fluid and cytoplasmic extracts derived from whole lung homogenates. Macrophage-inflammatory peptide 2 (MIP-2), tumor necrosis factor (TNF)-α, and monocyte chemotactic protein (MCP)-1 were assayed according to manufacturer's instructions with commercially available enzyme-linked immunosorbent assays (R&D Systems, Minneapolis, MN). The minimum detectable concentration of MIP-2, TNF-α, and MCP-1 was $<$ 1.5 pg/ml, $<$ 5.1pg/ml, and $<$ 2 pg/ml, respectively. Cytokine concentrations are reported as pg/ml of BAL fluid and as pg/μg of lung tissue.

Statistical Analysis

Statistical analyses were performed with GraphPad InStat version 3.01 for Windows NT (GraphPad Software, San Diego, CA) using an unpaired *t* test and unpaired ANOVA test.

Results

Administration of Clodronate via Various Routes Results in Different Levels of Depletion of Pulmonary Macrophages

To quantify the extent of tissue and alveolar macrophage depletion induced by clodronate treatment, alveolar macrophages were assessed by counting cells obtained by BAL. In addition, immunoreactive lung and liver macrophages were quantitated on tissue sections. Mice were treated with IT injection of liposomal clodronate, IV injection of liposomal clodronate, or combined IT+IV liposomal clodronate, and harvested 48 h later. Control mice received empty (PBS-containing) liposomes. Total cell counts in BAL from mice receiving clodronate were decreased compared with control mice (Figure 1A). Combination treatment with IT+IV clodronate resulted in a 75% reduction in the recovery of total cells in BAL fluid. IT or IV approaches alone resulted in 70% and 31% depletion, respectively.

Lavage macrophages displayed two distinct cell morphologies, intact and remnant macrophages. Remnant macrophages are defined by morphologic criterion that include visualization of a condensed nuclear body without a clear cytoplasm or limiting cell membrane. The number of remnant macrophages varied with the route of clodronate administration. Only a small number of remnant macrophages (2.2 ± 2.0% of the total macrophage population in BAL) were noted following liposomal PBS treatment (Figure 1B). Treatment with IV, IT, or IT+IV clodronate resulted in significantly higher percentages of remnant macrophages (38 ± 11%, 20 ± 7%, and 57 ± 2%, respectively) (Figure 1B). The number of intact macrophages obtained by lung lavage was lowest in combined IT+IV clodronate treatment, $1.4 \pm 0.4 \times 10^4$, which represented a 90% reduction compared with the PBS liposome–treated control (Figure 1C). A 66% reduction in intact macrophages was found in the IV clodronate group and a 77% reduction was found in the IT clodronate group.

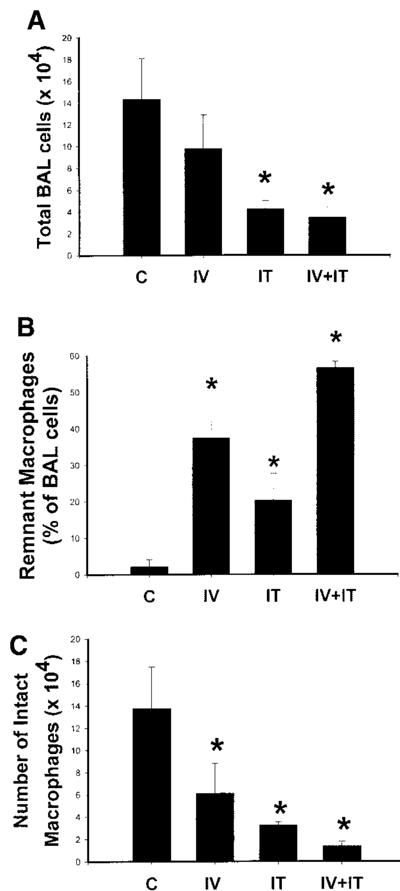

Figure 1. Depletion of lung macrophages by clodronate. (*A*) The total number of cells in BAL fluid 48 h after treatment with combined intravenous (IV) and/or intratracheal (IT) clodronate ($n = 4$ in each group) and controls treated with IT and IV injections of PBS-containing liposomes (C) ($n = 3$). (*B*) The number of remnant macrophages is shown as the percentage of the total BAL cells (*see* text for the criterion used to distinguish remnant macrophages). (*C*) The number of intact macrophages in BAL in response to clodronate treatment is shown. * indicates different from the PBS liposome–treated control, $P < 0.05$.

In addition to lung lavage, histologic sections of livers and lungs were examined to assess total tissue macrophage depletion following clodronate treatment. Figure 2 shows a representative example of liver and lung tissue from a mouse treated with empty liposomes compared with those of a mouse treated with IT+IV clodronate. Abundant Kupffer cells are identified in liver of control mice, but only scarce Kupffer cells are seen in clodronate-treated mice (Figure 2A). In lung sections, pulmonary macrophage depletion was also identified following IT+IV clodronate (Figure 2B).

Semiquanitative analysis of liver and lung tissue was performed to assess the reduction in immunoreactive tissue macrophages after clodronate treatment. Kupffer cells were reduced in number from 49 ± 4.3 cells per high-power field in PBS liposome treated mice to 3 ± 1.4 cells per high-power field in liver sections of mice treated with IT+IV clodronate ($P < 0.05$, $n = 3$ in each group). This finding indicates that there was a 94% reduction in Kupffer cells by clodronate treatment. In addition, reduced numbers of lung macrophages were demonstrated by analysis of lung tissue sections of mice treated with IT+IV clodronate. On lung sections, 9.5 ± 1.7 macrophages per high-power field were counted after treatment with PBS liposomes compared with 3.3 ± 0.4 macrophages per high-power field in lungs of mice treated with IT+IV clodronate, representing a 66% reduction in immunoreactive macrophages ($P < 0.05$, $n = 3$ in each group). Of particular note is that there was no evidence of tissue injury or inflammation in either the lungs or liver in response to the liposomal clodronate treatment.

Depletion of Macrophages with Combined IT+IV Clodronate Treatment Results in Attenuated Neutrophilic Alveolitis and Altered Cytokine Production following Inhaled LPS

Macrophage depletion induced by combined IT+IV clodronate markedly attenuates the extent of the acute inflammatory cell influx into the airways 4 h after inhaled LPS treatment (Figure 3). No significant neutrophilic alveolitis was

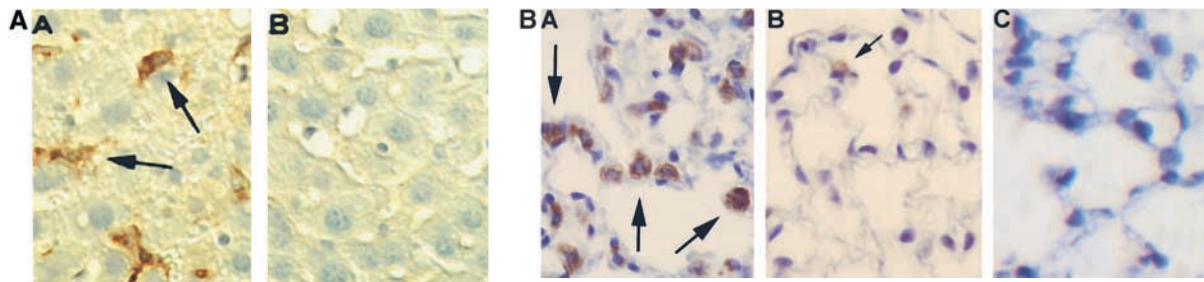

Figure 2. Depletion of tissue macrophages by clodronate. (*A*) Tissue sections are shown for liver following treatment with PBS liposomes (A) or combined IV+IT clodronate (B). Kupffer cells (*arrows*) were identified after immunostaining with F4/80 antibodies. Haemotoxylin was used as a counterstain. (*B*) Lung sections following treatment with PBS liposomes (A) or combined IV+IT clodronate (B). Lung macrophges were identified by immunostaining with lysozyme antibodies (*arrows*). A control section is shown (C) in which no primary antibody was added. Haemotoxylin was used as a counterstain. Magnification is 400×.

induced by liposome treatment, as judged by the observation that neutrophils accounted for only 1.1 ± 0.3 × 10^4 and 0.9 ± 0.2 × 10^4 of lavage cells from mice treated with empty liposomes and clodronate, respectively (n = 7–10, P = NS). After inhaled LPS, a substantial influx of neutrophils was found in control mice pretreated with empty liposomes (66.1 ± 6.9 × 10^4 neutrophils); however, treatment with IT+IV clodronate blunted this neutrophil influx by 80% (12.8 ± 2.9 × 10^4 neutrophils, $P < 0.0001$, n = 7–10 in each group). In contrast to these studies, IT clodronate by itself had no effect on total BAL cell counts (61.5 ± 14.9 × 10^4 cells in IT clodronate group versus 73.5 ± 6.1 × 10^4 cells in PBS liposome group, P = NS, n = 4–5) and the percentage of neutrophils was similar in the IT clodronate-treated mice compared with PBS liposome–treated mice after LPS treatment (95.5 ± 0.4% versus 86.6 ± 1.4%, P = NS, n = 4–5).

Treatment with combined IT + IV PBS or clodronate liposomes alone did not induce production of detectable TNF-α, MIP-2, or MCP-1 in lung lavage as assessed by enzyme-linked immunosorbent assay (not shown). In response to LPS treatment, however, PBS liposome–treated mice had much greater amounts of TNF-α in BAL fluid than clodronate-treated mice (1,353 ± 92 versus 175 ± 41 pg/ml, $P < 0.0001$, n = 13–14) (Figure 4A). Interestingly, MIP-2 levels in lung lavage were not different between control and clodronate-treated mice after inhaled LPS (304 ± 25 and 471 ± 60 pg/ml, P = NS, n = 13,14) (Figure 4A); however, MIP-2 levels were decreased in lung tissue homogenates of IT+IV clodronate-treated mice compared with PBS liposome–treated mice following LPS inhalation (78 ± 10 and 289 ± 42 μg/g, respectively, $P < 0.01$, n = 13–14) (Figure 4B). In contrast, MCP-1 concentrations in lung tissue homogenates of PBS liposome–treated controls and clodronate-treated mice was not different (659 ± 129 and 838 ± 198 μg/g, respectively, P = NS, n = 13–14) (Figure 4B). Following inhaled LPS, however, BAL MCP-1 levels were increased in clodronate-treated mice compared with mice treated with PBS liposomes (417 ± 120 and 72 ± 44 pg/ml, respectively, P = 0.03, n = 13–14) (Figure 4A).

Depletion of Macrophages Results in Attenuated NF-κB Activation in Whole Lung Tissue following Inhaled LPS

We evaluated the effect of macrophage depletion with IT+IV clodronate on global lung NF-κB activation in response to inhaled LPS. NF-κB DNA binding activity was detected by electromobility shift assays (EMSA) performed on nuclear extracts derived from whole lung tissues. Macrophage-depleted mice had attenuated DNA binding activity of both the heterodimer (RelA/p50) and homodimer (p50/p50) bands in response to inhaled LPS treatment compared with control mice treated with PBS liposomes (Figure 5A). Unstimulated mouse lungs exhibit minimal NF-κB activation by EMSA (data not shown).

Using laser densitometry, we compared the intensity of the RelA/p50 heterodimer bands on EMSA from lungs of mice treated with PBS liposomes or IT+IV clodronate followed by inhaled LPS. We measured the RelA/p50 band because the RelA component of NF-κB contains a transactivation domain whereas the p50 component does not (16), and therefore RelA is thought to stimulate the transcriptional activity induced by NF-κB binding. The density of the RelA/50 heterodimer band from control lungs in each experiment was defined as 100% and the density of the RelA-containing band from IT+IV clodronate-treated mice was measured as a percentage of the mean control density in each experiment. Clodronate treatment resulted in a 65% reduction in

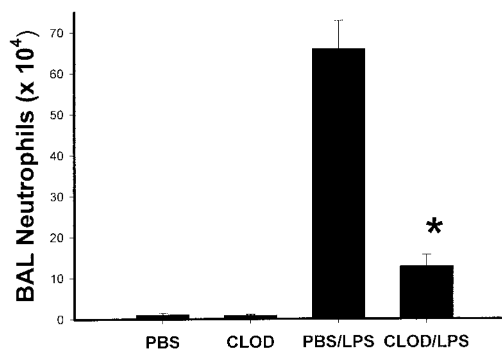

Figure 3. Macrophage depletion attenuates LPS-induced neutrophil recruitment: Total neutrophil counts in BAL fluid are shown after combined IT+IV treatment with PBS-containing liposomes (PBS) or clodronate (CLOD). Four hours after exposure to aerosolized LPS, neutrophil influx was reduced in mice previously treated with clodronate (CLOD/LPS) compared with mice treated with PBS liposomes (PBS/CLOD). * indicates $P < 0.05$, n = 7–10.

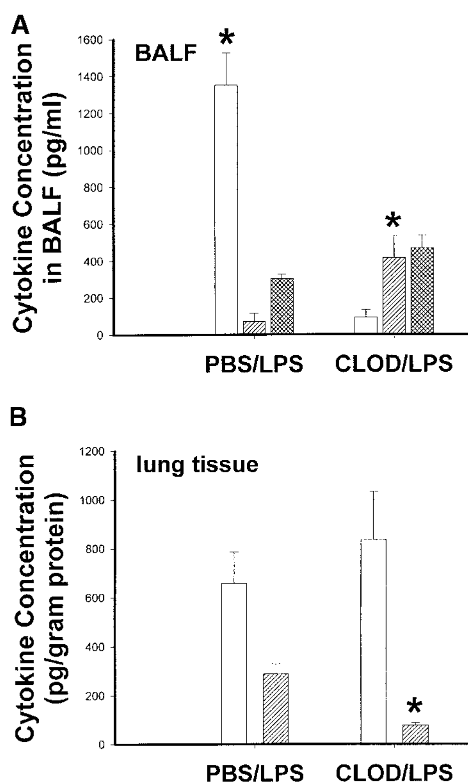

Figure 4. Macrophage depletion attenuates LPS-induced TNF-α production and tissue MIP-2 levels. (*A*) Concentrations of TNF-α (*open bars*), MCP-1 (*striped bars*), and MIP-2 (*hatched bars*) in cell-free BAL fluid (BALF) of mice exposed to aerosolized LPS. These cytokines were not detected in PBS liposome– or clodronate-treated mice without LPS treatment. (*B*) MCP-1 (*open bars*) and MIP-2 (*striped bars*) concentrations in lung tissue homogenates are shown and normalized for total protein. * Indicates different from the PBS liposome samples, $P < 0.05$, $n = 13$–14.

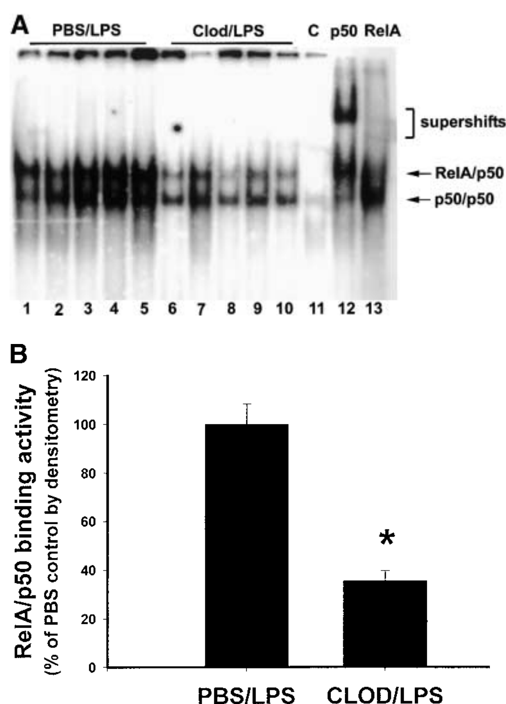

Figure 5. Macrophage depletion attenuates lung NF-κB activation after inhaled LPS. (*A*) The results of an EMSA obtained from nuclear extracts from lung tissue after treatment with PBS-containing liposomes (*lanes 1–5*) and IT+IV clodronate (*lanes 6–10*) in response to exposure to aerosolized LPS. The position of the RelA/p50 heterodimer and the p50 homodimer bands were determined by supershift studies that utilized antibodies to p50 and RelA (*lanes 12* and *13*). Both bands could be specifically competed with excess cold (unlabeled) probe (C) (*lane 11*). (*B*) The relative density of RelA/p50 bands on EMSA from lung tissue nuclear extracts of mice treated with PBS-containing liposomes or IT+IV clodronate before aerosolized LPS. Mean density of bands from PBS liposome–treated mice in each experiment is defined as 100% and density of bands from clodronate-treated mice is expressed as a percentage of the mean density of the PBS liposome control. * Indicates significantly different from the PBS liposome group, $P < 0.05$, $n = 13$–14.

LPS-induced NF-κB activity as defined by RelA/p50 band density ($P < 0.0001$, $n = 13$–16) (Figure 5B).

Depletion of Lung Macrophages Is Required to Block NF-κB Activation following Intraperitoneal Injection of LPS

To better define the role of macrophages in regulating lung inflammation in response to systemic LPS, we used a model of lung inflammation induced by IP injection of LPS (5 μg/g). Mice were treated with clodronate by IV injection alone or IT+IV clodronate injections 48 h before IP LPS. Combined treatment with IT+IV clodronate decreased neutrophil recruitment into the lavagable airspace in response to LPS treatment by 95% (Figure 6). Also, at 90 min after IP LPS there was a marked attenuation of NF-κB–binding activity in nuclear extracts of lung tissue from mice treated with IT+IV clodronate (Figure 7). Interestingly, LPS-induced liver NF-κB activation was not affected by clodronate treatment (not shown). In contrast, after IP injection of LPS, mice treated with IV clodronate alone showed no differences in BAL neutrophil numbers compared with control mice treated with PBS liposomes. In addition, no differences were detected in NF-κB–binding activity in lung or liver tissue between the two groups (data not shown). Similar to the model of direct airway stimulation by inhaled LPS, systemic LPS requires macrophages to produce lung inflammation. Additionally, combined treatment by IT+IV clodronate was required to limit LPS-induced inflammation in both models.

Discussion

Mononuclear phagocytes are thought to have a prominent role in initiating inflammation because of an impressive and diverse repertoire of function. In addition to locomotion, phagocytosis, and microbiocidal activities, resident and infiltrating macrophages secrete a variety of chemokines and cytokines that result in leukocyte recruitment to an inflammatory focus and enhance immune responses by cooperating with other components of the immune system (17–19). In liver, Kupffer cells perform a similar function by clearing intraperitoneal and blood-borne toxins and re-

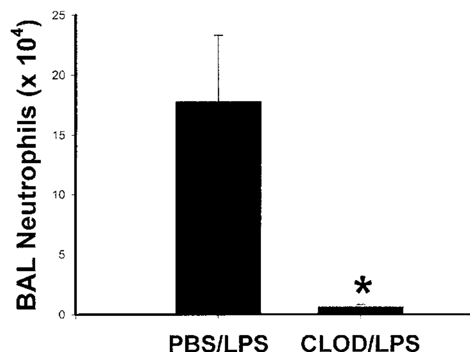

Figure 6. Macrophage depletion attenuates neutrophil alveolitis following IP LPS. Total neutrophil counts in BAL fluid are shown after combined IT+IV PBS liposome (PBS) or clodronate (CLOD) treatment, followed by IP injection of LPS (5 μg/g). * indicates difference from PBS/LPS group, $P < 0.05$, $n = 5$ in each group.

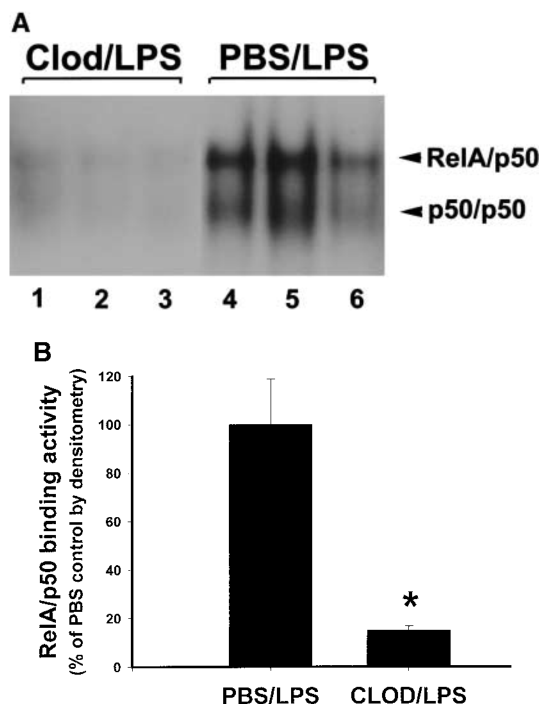

Figure 7. Macrophage depletion abrogates lung NF-κB activation following IP LPS. (*A*) The results of an EMSA are shown using nuclear extracts from lung tissue. Mice were treated with IT+IV clodronate (*lanes 1–3*) or PBS liposomes (*lanes 4–6*). Forty-eight hours later, mice were treated with IP injection of LPS (5 μg/g) and harvested 90 min after LPS injection. (*B*) The relative density of the RelA/p50 bands in these experiments are shown on this figure. Mean density of bands from PBS liposome–treated mice in each experiment is defined as 100% and density of bands from clodronate-treated mice is expressed as a percentage of the mean density of the PBS liposome control. * indicates significantly different from the PBS/liposome group, $P < 0.05$, $n = 9$–13.

leasing proinflammatory cytokines and tissue mediators that modulate the systemic response to intraperitoneal sepsis (19).

To examine the role of macrophages in the pathogenesis of neutrophilic lung inflammation in response to LPS, macrophages were eliminated by treatment with liposome-encapsulated clodronate. We observed that the extent of macrophage depletion is dependent upon the route of clodronate administration and that combined IT+IV clodronate achieves the most impressive depletion of pulmonary macrophages compared with either route alone. This combined route reliably resulted in a 90% reduction in the number of intact macrophages present in lung BAL fluid compared with control animals and substantially depleted macrophages in lung and liver tissue. We postulate that in the lung, combined IT+IV clodronate induces apoptosis of both alveolar and interstitial lung macrophages.

Elimination of macrophages with combined IT+IV clodronate treatment results in decreased lung NF-κB activity, neutrophilic alveolitis, and pulmonary TNF-α production following exposure to aerolized LPS. Lung tissue–bound MIP-2 was also decreased, although macrophage depletion did not result in decreased levels of MIP-2 in BAL fluid. The most likely explanation for this discrepancy is that MIP-2 is tightly associated with tissue-bound heparin moieties. Surprisingly, MCP-1 levels were increased in BAL fluid, which may represent a compensatory regulatory mechanism that is related to extensive macrophage depletion. In contrast to the effects of combined IT+IV clodronate, IT clodronate alone had no effect on pulmonary inflammation associated with exposure to aerosolized LPS. Our studies also show that combined IT+IV clodronate was effective in preventing neutrophil recruitment to the lung and blocking activation of NF-κB in the lung following IP injection of LPS, whereas IV clodronate alone had no effect on pulmonary inflammation associated with IP LPS treatment. Together, these data suggest either that LPS-induced lung inflammation is a consequence of events that occur in both the pulmonary and extrapulmonary macrophage pool or that a near-complete depletion of viable macrophages in the lung is required to inhibit LPS-induced lung inflammation.

Our finding that macrophages are essential for maximal NF-κB activity is consistent with that of other investigators. Lentsch and coworkers (21) showed that macrophage depletion by IT administration of clodronate results in a marked reduction of NF-κB–binding activation, reduced TNF-α, MIP-2, and ICAM-1 gene expression in lung tissue, and decreased lung inflammation and injury following intratracheal instillation of IgG complexes. Our data, along with this study, indicate that macrophages are essential for maximal lung inflammation as defined by NF-κB activation in lung tissue, chemokine and cytokine production, and recruitment of neutrophils. Although our data are consistent with the hypothesis that macrophages alone are sufficient to generate the entire extent of the inflammatory response, it is much more likely that macrophages initiate the response and that other cell types, including rapidly infiltrating neutrophils, contribute to the intensity or duration of the acute inflammatory response to endotoxin.

Numerous studies have examined the role of macrophages in infectious models of lung inflammation using inoculation of bacteria such as *Pseudomonas aeruginosa* (11, 12, 22), *Klebsiella pneumoniae* (9), and *Pneumocystis carinii* (10) in clodronate-treated animals. These studies have

reported varying effects of macrophage depletion on the development of neutrophilic lung injury and tissue expression of inflammatory cytokines TNF-α, MIP-2, KC, and cytokine-induced neutrophil chemoattractant (CINC). Although some investigators have found decreased expression of TNF-α, CINC, and MIP-2 in association with decreased neutrophilic influx in *P. aeruginosa* pneumonia (12), other investigators have described increased or persistent, albeit delayed, neutrophil influx into the lungs following bacterial inoculation (9). Several studies have described impaired bacterial clearance with increased bacterial load both locally in the lungs and systemically (9–10). We speculate that impaired clearance of bacteria is a persistent stimulus for neutrophil influx that may obviate the role of macrophages in phagocyte recruitment through inherently redundant arms of the inflammatory cascade generated either by neutrophils or by other lung cell types.

Interestingly, we found that IV clodronate treatment, which results in substantial Kupffer cell depletion, did not protect against either lung or liver inflammation following intraperitoneal LPS. Similarly, Iimuro and colleagues (23) found no corresponding decline in hepatic TNF-α production following intravenous LPS administration to gadolinium-treated animals. These findings are in contrast to studies that examined the role of Kupffer cells in intraperitoneal sepsis using gadolinium chloride before bile duct ligation (24) or cecal ligation and puncture (20, 25). These studies described reduced hepatic expression of the inflammatory cytokines TNF-α, interleukin-1β, and interleukin-6, and reduced mortality in Kupffer cell–depleted animals. The discrepancy between the LPS models and those of bile duct ligation or cecal ligation and puncture may indicate that tissue distribution of purified endotoxin is more extensive than bacterial-associated endotoxin. It is possible that purified LPS injections localize to and activate hepatocytes while bacterial clearance is dependent on phagocytosis by Kupffer cells (26).

In summary, we conclude that macrophage depletion with clodronate reduces NF-κB activation, production of TNF-α and chemokine, and neutrophilic lung inflammation in response to Gram-negative bacterial endotoxin. We have shown that combined IT+IV clodronate treatment is most efficacious in blocking the development of neutrophilic lung inflammation in response to either IP LPS or exposure to an LPS aerosol. In our studies, IT clodronate did not block inflammation caused by exposure to a LPS aerosol and IV clodronate did not block inflammation caused by endotoxemia. These data, together, seem to suggest that widespread and efficient targeting of macrophages is necessary to attenuate the response to endotoxin.

Acknowledgments: This study was supported by the Cystic Fibrosis Foundation; the U.S. Department of Veterans Affairs; and Grant HL 61419 from the National Heart, Lung, and Blood Institute, National Institutes of Health.

References

1. van Rooijen, N., N. Kors, N. van der Ende, and M. Dijkstra. 1990. Depletion and repopulation of macrophages in spleen and liver of rat after intravenous treatment with liposome-encapsulated dichloromethylene disphosphonate. *Cell Tissue Res.* 260:215–222.
2. van Rooijen, N., and R. van Nieuwmegen. 1984. Elimination of phagocytic cells in the spleen after intravenous injection of liposome-encapsulated dichloromethylene diphosphonate: an enzyme-histochemical study. *Cell Tissue Res.* 238:355–358.
3. van Rooijen, N., and A. Sanders. 1994. Lipsome mediated depletion of macrophages: mechanism of action, preparation of liposomes and applications. *J. Immunol. Methods* 174:83–93.
4. Schmidt-Weber, C. B., M. Rittig, E. Buchner, I. Hauser, I. Schmidt, E. Palombo-Kinne, F. Emmrich, and R. W. Kinne. 1996. Apoptotic cell death in activated monocytes following incorporation of clodronate-liposomes. *J. Leukoc. Biol.* 60:230–244.
5. van Rooijen, N., A. Sanders, and T. K. van den Berg. 1996. Apoptosis of macrophages induced by liposome-mediated intracellular delivery of clodronate and propamidine. *J. Immunol. Methods* 193:93–99.
6. Naito, M., H. Nagai, S. Kawano, H. Umezu, H. Zhu, H. Moriyama, T. Yamamoto, H. Takatsuka, and Y. Takei. 1996. Liposome-encapsulated dichloromethylene diphosphonate induces macrophage apoptosis in vivo and in vitro. *J. Leukocyte Biol.* 60:337–344.
7. Berg, J. T., S. T. Lee, T. Thepen, C. Y. Lee, and M. F. Tsan. 1993. Depletion of alveolar macrophages by liposome-encapsulated dichloromethylene diphosphonate. *J. Appl. Physiol.* 74:2812–2819.
8. Thepen, T., N. van Rooijen, and G. Kraal. 1989. Alveolar macrophage elimination in vivo is associated with an increase in pulmonary immune response in mice. *J. Exp. Med.* 170:499–509.
9. Broug-Holub, E., G. Toews, J. F. van Iwaarden, R. M. Strieter, S. L. Kunkel, R. Paine, and T. J. Standiford. 1997. Alveolar macrophages are required for protective pulmonary defenses in murine Klebseilla pneumonia: elimination of alveolar macrophages increases neutrophil recruitment but decreases bacterial clearance and survival. *Infect. Immun.* 65:1139–1146.
10. Limper, A. H., J. S. Hoytes, and J. E. Standing. 1997. The role of alveolar macrophages in Pneumocystis carinii degradation and clearance from the lung. *J. Clin. Invest.* 99:2110–2117.
11. Kooguchi, K., S. Hashimoto, A. Kobayashi, Y. Kitamura, I. Kudoh, J. Wiener-Kronish, and T. Sawa. 1998. Role of alveolar macrophages in initiation and regulation of inflammation in Pseudomonas aeruginosa pneumonia. *Infect. Immun.* 66:3164–3169.
12. Hashimoto, S., J.-F. Pittet, K. Hong, H. Folkesson, G. Bagby, L. Kobzik, C. Frevert, K. Watanabe, S. Tsurufuji, and J. Weiner-Kronish. 1996. Depletion of alveolar macrophages decreases neutrophil chemotaxis to Pseudomonas airspace infections. *Am. J. Physiol. Lung Cell. Mol. Physiol.* 270:L819–L828.
13. Sadikot, R. T., E. D. Jansen, T. R. Blackwell, O. Zoia, F. E. Yull, J. W. Christman, and T. S. Blackwell. 2001. High dose dexamethasone accentuates NF-κB activation in endotoxin-treated mice. *Am. J. Respir. Crit. Care Med.* 164:873–878.
14. Deryckere, F., and F. Gannon. 1994. A one-hour minipreparation technique for extraction of DNA binding proteins from animal tissues. *Biotechniques* 16:405.
15. Bradford, M. M. 1976. A rapid and sensitive method for the quantification of microgram quantities of protein utilising the principle of protein-dye binding. *Anal. Biochem.* 72:248–254.
16. Baeuerle, P. A. 1991. The inducible transcription activator NF-κB: regulation by distinct protein subunits. *Biochim. Biophys. Acta* 1072:63–80.
17. Henson, P. M., D. W. H. Riches, G. S. Worthen, P. E. Parsons, and D. E. Doherty. 1994. LPS and cytokines in lung injury. *In* Endotoxin and the Lungs. K. L. Brigham, editor. Marcel Dekker, New York. 267–304.
18. Bezdicek, P., and R. G. Crystal. 1997. Pulmonary macrophages. *In* The Lung: Scientific Foundations. R. G. Crystal and J. B. West, editors. Lippincott-Raven, Philadelphia. 859–875.
19. Unanue, E. R., and P. M. Allen. 1987. The basis for the immunoregulatory role of macrophages and other accessory cells. *Science* 236:551–557.
20. Callery, M. P., T. Kamei, and W. Flye. 1990. Kupffer cell blockade increases mortality during intra-abdominal sepsis despite improving systemic immunity. *Arch. Surg.* 125:36–40.
21. Lentsch, A. B., B. J. Czermak, N. M. Bless, N. van Rooijen, and P. A. Ward. 1999. Essential role of alveolar macrophages in intrapulmonary activation of NF-κB. *Am. J. Respir. Cell Mol. Biol.* 20:692–698.
22. Cheung, D. O. Y., K. Halsey, and D. P. Speert. 2000. Role of pulmonary alveolar macrophages in defense of the lung against Pseudomonas aeruginosa. *Infect. Immun.* 68:4585–4592.
23. Iimuro, Y., M. Yamamoto, H. Kohno, J. Itakura, H. Fujii, and Y. Matsumoto. 1994. Blockade of liver macrophages by gadolinium chloride reduces lethality in endotoxemic rats- analysis of mechanisms of lethality in endotoxemia. *J. Leukoc. Biol.* 55:723–728.
24. Kennedy, J. A., H. Lewis, W. D. B. Clements, S. J. Kirk, G. Campbell, M. I. Halliday, and B. J. Rowlands. 1999. Kupffer cell blockade, tumour necrosis factor secretion and survival following endotoxin challenge in experimental biliary obstruction. *Br. J. Surg.* 86:1410–1414.
25. Koo, D. J., I. H. Chaudry, and P. Wang. 1999. Kupffer cells are responsible for producing inflammatory cytokines and hepatocellular dysfunction during early sepsis. *J. Surg. Res.* 83:151–157.
26. Opal, S. M. 1999. The value of animal models in endotoxin research. *In* Endotoxin in Health and Disease. H. Brade, S. M. Opal, S. N. Vogel, and D. C. Morrison, editors. Marcel Dekker, New York. 809–816.